



OPEN Metabolomic profiling of serum alterations and biomarker discovery in feline hepatic liposis

Xingbo Wang^{1,2}, Ruru Xu^{1,2}, Weizhe Yan^{1,2}, Kexin Wang¹, Xichun Wang¹, Shibin Feng¹ & Chang Zhao¹✉

Feline hepatic lipodosis (FHL) is a common liver dysfunction caused by metabolic disorders. The objective was to evaluate the metabolic alteration in the cats of FHL and to identify biomarkers that can serve as biomarker for FHL. Differential metabolites in the serum of spontaneous FHL cats (FS, $n=12$) and healthy cats (CS group, $n=12$) were analyzed using GC/MS metabolomics. Differential metabolites with diagnostic significance were identified through receiver operating characteristic (ROC) curves. The expression level of the differential metabolite 2-hydroxybutyric acid (2-HB) was detected in the serum of the FS and CS groups, and biomarker were established. The biomarker efficacy of 2-HB for FHL was verified using serum samples from cats with FHL caused by different etiologies (F, $n=10$) and healthy cats (C, $n=50$). There were 13 significantly different metabolites between the CS and FS groups ($VIP>1$, $P<0.05$) with the area under the ROC curve (AUC) greater than 0.70. The AUC for serum 2-HB was 0.90 (95% confidence interval 0.767–1.000, $P<0.001$), with an optimal critical value of 564.8 ng/L. By randomly detecting serum 2-HB in groups F and C (the optimal cut-off value is 564.8 ng/L), the detection rate for FHL diagnosis was 100% and the false positive rate was 0%. In cats with FHL, metabolic changes occur in amino acids, nucleotide sugars, glycerophospholipids, phenylalanine, galactose, alpha-linolenic acid, and glycerides. A serum 2-HB level greater than 564.8 ng/L serves as a biomarker for FHL.

Keywords Feline hepatic lipodosis, Metabolites, Diagnostic biomarkers, 2-Hydroxybutyric acid

Cats are obligate carnivores that rely on nutrients found in animal tissues and have evolved unique characteristics in protein and fat metabolism¹. Cats maintain high levels of protein oxidation and gluconeogenesis, and are unable to adapt to reduced protein intake, resulting in higher requirements for essential amino acids and fatty acids. Unlike most other species, cats are unable to preserve certain amino acids, including methionine, cysteine, taurine, and arginine. Therefore, cats require a higher dietary intake of protein and B vitamins, and are prone to negative energy balance over time due to decreased food intake¹. This unique dietary requirement makes cats more susceptible to Hepatic Lipodosis. The characteristics of Feline Hepatic Lipodosis (FHL) include excessive accumulation of triglycerides (TG) in liver cells, secondary damage to liver function and intrahepatic cholestasis, fatty changes in liver cells, vacuolization, and infiltration of monocytes². The etiology of FHL may be anorexia caused by diseases or special conditions, with no preference for gender or breed, and occurring at different ages, though most cases are seen in obese cats³. FHL typically presents with early clinical symptoms such as drowsiness, decreased appetite, weight loss, and liver enlargement in the early stages. The response of cats to anorexia is unique and severe, and the metabolic changes behind this disease are complex, with the pathogenesis still unclear. However, in clinical, if FHL is detected early and treated appropriately, the prognosis is generally positive; if not detected early, the prognosis may be more severe². Therefore, understanding the metabolic characteristics of FHL can help clarify its pathogenesis and facilitate the screening of diagnostic biomarker.

Metabolomics is a method for identifying and quantitatively detecting metabolites in the body, used to study the dynamic metabolic processes of biological systems affected by genetic or disease factors⁴. Metabolomics techniques have been widely applied in disease-related research, but little is known about the metabolic profile of domestic cats^{5–7}. Currently, serum metabolomics analysis has been conducted on overweight and obese cats⁸. The analysis shows that as cats lose weight, the metabolite profile constantly changes, and most lipid metabolites decrease with weight loss. However, ketone bodies and small lipid particles increase with weight loss. Most carbohydrate metabolites also decrease with weight loss, while the results for protein metabolites vary. It

¹College of Animal Science and Technology, Anhui Agricultural University, Hefei, China. ²Xingbo Wang, Ruru Xu and Weizhe Yan contributed equally to this work. ✉email: chang_zhao@ahau.edu.cn

was found that the metabolic mediators of inflammation, oxidative stress, exogenous hormones, and insulin resistance decrease with weight loss. This study identified biomarkers for reduced food intake and weight loss in cats, including reduced inflammatory markers and changes in macronutrient metabolism⁸. The identification of biomarkers for cat weight loss is significance in improving metabolism and reducing clinical symptoms in obese cats, and can to some extent prevent the occurrence of FHL⁸. The Pallotto team has provided a better understanding of the metabolic patterns of feline animals. Based on this, the present study will analyze the serum metabolomics of FHL, laying the foundation for identifying therapeutic targets and understanding its pathogenesis. Additionally, ROC analysis will be used to screen for differential metabolites that can serve as biomarker.

Materials and methods

Animals and ethics approval

This study was conducted in accordance with the ARRIVE guidelines (<https://arriveguidelines.org>) to ensure rigorous standards in animal research reporting. All procedures were performed following relevant ethical guidelines and regulations. The study was approved by the Animal Welfare and Research Ethics Committee of Anhui Agricultural University, China (Approval Number: 2021012-1). All cats were clinical cases treated at Anhui Agricultural University Teaching Animal Hospital, Daqing Renxin Pet Hospital, and Daqing Kang'an Pet Hospital. Written, informed consent was obtained from all cat owners prior to study enrolment of their cats in the study. When selecting the experimental animals, we excluded cats with other diseases and complications arising from FHL through complete blood count, serum biochemical examinations, and B-ultrasounds. Based on clinical symptoms, liver biopsy and ultrasound testing confirm FHL (FS group, $n = 12$; the detection results are shown in Supplementary Fig. 1). The healthy cats were identified through life history, serum biochemical indicators, and ultrasound testing (CS group, $n = 12$).

Sample collection

Venous blood was collected from the forelimbs of the fasting cats prior to feeding all experimental cats in the morning. A fully automatic blood cell analyzer (for animal use) was used to measure various blood routine indicators. Simultaneously, the venous blood was placed in centrifuge tubes without anticoagulants. The samples were kept at 4 °C for 2 h and then centrifuged at 3000 r/min for 10 min. The serum samples were prepared from the supernatant, and the biochemical indicators of the CS and FS groups were measured using a fully automatic biochemical analyzer. The samples were stored at -80 °C for metabolomics detection.

For general anesthesia in cats, subcutaneous injection of atropine sulfate (0.02–0.04 mg/kg) and intravenous injection of anesthetic propofol (6–8 mg/kg) were administered 15 min before surgery. A 16G, 20 centimeter long biopsy needle (Pro MAG biopsy needle; Argon Medical Device) was used for percutaneous ultrasound-guided liver biopsy under general anesthesia. Liver biopsy tissue were preserved using paraformaldehyde. All experimental cats did not show any other complications after liver biopsy.

Complete blood count and serum biochemical indicators analysis

The Complete Blood Count (CBC) and blood biochemical indicators are measured using a fully automated blood cell analyzer and a fully automated biochemical analyzer, both manufactured by Mindray in Shenzhen, China. Complete blood count parameters including Red Blood Cell Count (RBC), Hemoglobin (HGB), Hematocrit (HCT), Mean Corpuscular Volume (MCV), Mean Corpuscular Hemoglobin (MCH), Mean Corpuscular Hemoglobin Concentration (MCHC), Red Blood Cell Distribution Width (RDW), White Blood Cell Count (WBC), Lymphocyte (Lym), Monocytes (Mono), Neutrophil (NE), Lymphocyte Ratio (LYMPH%), Monocyte Ratio (MONO%), Neutrophil Ratio (NEUT%), Eosinophils Ratio (EO%), Platelet Count (PLT), Mean Platelet Volume (MPV), Platelet Distribution Width (PDW), Plateletcrit (PCT), while serum biochemical parameters including Alkaline Phosphatase (ALP), Alanine Transferase (ALT), Aspartate Aminotransferase (AST), Total Cholesterol (TC), Triglycerides (TG), Creatine Kinase (CK), Serum Bilirubin (TBIL-V), Low-Density Lipoprotein Cholesterol (LDL-C), Phosphorus (P), High-Density Lipoprotein Cholesterol (HDL-C), Gamma-Glutamyl Transferase (γ -GGT), Total Protein (TP), Albumin (ALB), Globulin (GLB), Albumin/Globulin (A/G), Blood Urea Nitrogen (UREA), Amylase (a-AMY), Calcium (Ca) and Creatinine (CREA-S) were measured using commercial kits and instruments from our previous research⁹.

Non targeted metabolomics methods

The screening and analysis of metabolites were conducted by BIOTREE PROFILE Co. Ltd in Shanghai, China. We will briefly describe the method.

Metabolite extraction

Add 400 μ L of methanol (including internal standard ribose) to 100 μ L of serum sample, vortex for 30 s, sonicate at 4 °C for 10 min, centrifuge at 4 °C at 12,000 rpm (centrifugal force of 13800 ($\times g$), radius of 8.6 cm) for 15 min. Take the supernatant. Mix 80 μ L of supernatant from each sample to create Quality Control samples, and dry the extract in a vacuum concentrator. Add 30 μ L of methoxamine salt reagent (methoxamine hydrochloride, dissolved in pyridine 20 mg/mL) to the dried metabolite and incubate at 80 °C in an oven for 30 min. Add 40 μ L (trimethylsilyl) trifluoroacetamide (containing 1% trimethylchlorosilane, v/v) to each sample and incubate the mixture at 70 °C for 1.5 h; Cool to room temperature and add 5 μ L of fatty acid methyl esters (dissolved in chloroform) to the mixed sample. Samples were analyzed randomly.

Metabolite identification

Agilent 7890 gas chromatography-time-of-flight mass spectrometer was used for metabolite identification (Agilent DB-5MS capillary column, 30 m x 250 μ m x 0.25 μ m, J&W Scientific, Folsom, CA, USA). The specific analysis conditions for GC/TOF/MS were as follows: Sample volume was 1 μ L in splitless mode; front inlet septum purge flow was 3 mL/min; carrier gas was helium with a column flow of 1 mL/min; Temperature Ramp is 50 °C, held for 1 min, ramped to 310 °C at a rate of 20 °C/min, and held for 6 min; front injection temperature was 280 °C; transfer line temperature was 280 °C; ion source temperature was 250 °C; electron energy was –70 eV; mass range was 50–500 m/z; acquisition rate was 12.5 spectra per second; and solvent delay was 4.88 min.

Bioinformatics analysis of differential metabolites

Mass spectrometry data were processed using ChromaTOF software (V4.3x, LECO) for peak extraction, baseline correction, deconvolution, peak integration, and alignment. Qualitative analysis of substances was conducted using the LECO Fiehn Rtx5 database, which includes mass spectrometry and retention time index matching. The raw data set comprises 4 quality control (QC) samples and 24 experimental samples, from which a total of 479 peaks were initially extracted. The preprocessing steps mainly involved filtering outlier values, handling missing values through imputation, and standardizing the data. After completing these preprocessing steps, 336 peaks were retained for further analysis^{10,11}. Peaks with detection rates below 50% or RSD > 30% were removed from QC samples. Using SIMCA software (V16.0.2, Sartorius Stedim Data Analytics AB, Umea, Sweden), Centralize (CTR) formatting of data and subjected to automatic modeling and analysis. Use Principal Component Analysis (PCA) to analyze and compare the overall distribution of samples, determine the differences between groups, and determine the principal components. Using orthogonal partial least squares discriminant analysis (OPLS-DA) statistical method to analyze the results, select orthogonal variables in metabolites that are not related to categorical variables, and analyze non orthogonal variables and orthogonal variables separately. Combine the results of unit variable and multivariate statistical analysis to screen for differential metabolites. The Variable Importance for the Projection (VIP) obtained from the OPLS-DA model is usually considered to have a significant contribution in model interpretation when the metabolite VIP > 1. This experiment used VIP > 1 and $P < 0.05$ as criteria to screen for significantly different metabolites. Calculate the Euclidean distance matrix for quantitative values of differential metabolites clustered using complete linkage method. Using the Kyoto Encyclopedia of Genes and Genomes (KEGG) Pathway Database (<http://www.kegg.jp/kegg/pathway.html>). Based on the functional information of genes and genomes, and using metabolic reactions as clues, possible metabolic pathways and regulatory proteins were linked to illustrate cellular physiological and biochemical processes based on gene and genome functional information. The Rich Factor, calculated as the ratio of annotated differential metabolites to all metabolites in a pathway, was derived from enrichment results in KEGG metabolic pathways. Each distinct qualitative differential metabolite was analyzed with a ROC curve, calculating the area under the curve (AUC) was calculated, along with the Youden index.

Validation of serum 2-HB for diagnosis of FHL

We randomly gathered clinical samples from cats diagnosed with feline hepatic lipidosis (FHL) at animal hospitals located in Hefei, Anhui Province, and Daqing, Heilongjiang Province, forming the F group ($n = 10$). Concurrently, we randomly selected healthy cats without any known diseases to create Group C ($n = 50$). Serum samples were collected from all 60 cats. The samples were then randomized, and a blind test was conducted to detect serum 2-HB levels in each sample. The presence of FHL was determined based on the 2-HB detection results. Finally, the positive detection rate was calculated by dividing the number of positive samples by the total number of samples tested.

Statistical analysis

Statistical analysis was performed using IBM SPSS 18.0. Student's t-tests were utilized to compare differences in baseline indicators between the two groups. Data were presented as mean \pm standard deviation as $P > 0.05$ as no significant difference, $P < 0.05$ indicates significant, and $P < 0.01$ indicated high significance. Column charts and ROC curves were generated using GraphPad Prism version 8.0 software to determine the optimal cutoff values for biomarkers, and to calculate sensitivity and specificity.

Results

Complete blood count and serum biochemical indicators analysis

The results indicated that compared to the CS group, PLT in the FS group decreased ($P < 0.05$, Supplementary Fig. 1), while no significant differences were observed in other blood routine indicators (Supplementary Table 1). The results of biochemical indicators are shown in Fig. 1, revealing that compared with the CS group, the FS group exhibited significantly elevated serum levels of ALP, ALT, AST, TC, TG, and CK ($P < 0.05$). Additionally, serum levels of TBIL-V and LDL-C were significantly increased ($P < 0.01$), while levels of CREA-S, P, and HDL-C were significantly decreased ($P < 0.05$). No statistically significant changes were observed in other indicators (Supplementary Table 2).

Multivariate statistical analysis of serum metabolism

PCA analysis was conducted on samples from the FS and CS groups, and the results are depicted in Fig. 2. Both groups of samples were found to be predominantly within the 95% confidence interval. Utilizing OPLS-DA analysis (Fig. 3a), a distinct separation trend was observed between the two groups, indicating significant metabolic differences. The model underwent 200 permutation tests, with results for the permutation test of the CS group on the FS group OPLS-DA model are shown in Fig. 3b, $R^2Y = 0.38$, $Q^2 = -0.73$. The permutation retention was equal to 1, indicating an original model $R^2Y = 0.661$ and $Q^2 = 0.407$. As permutation retention

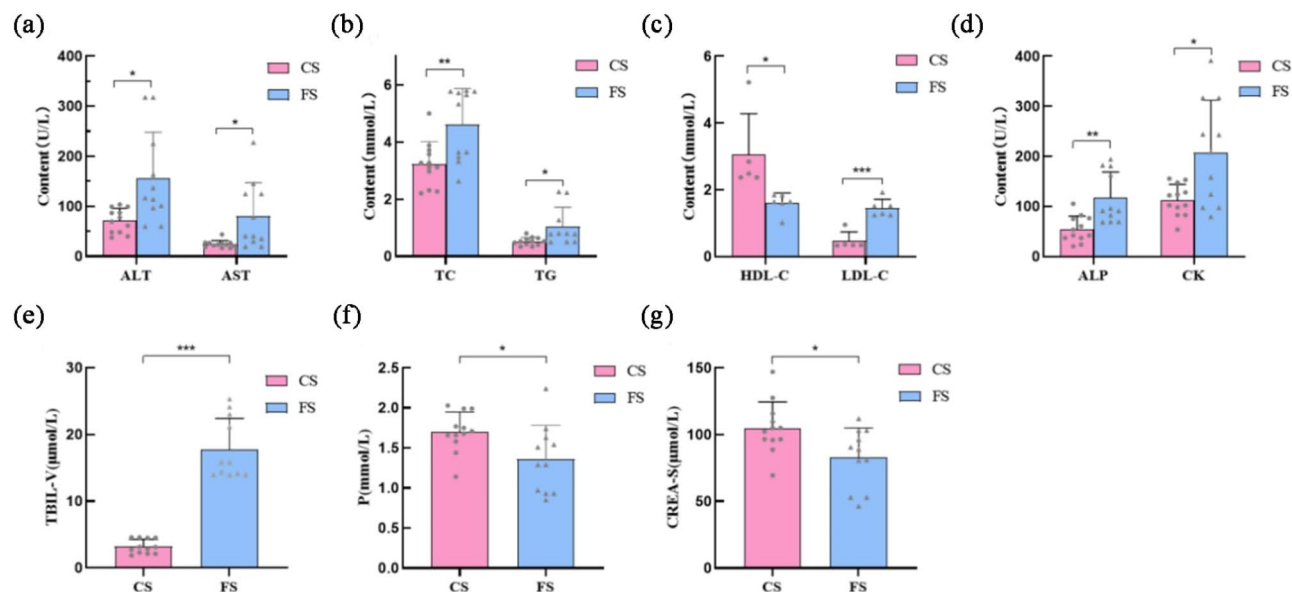


Fig. 1. Serum biochemical parameter levels in CS and FS groups. *Note:* (a) is the contents of Alanine aminotransferase (ALT) and Aspartate aminotransferase (AST) in the serum of the CS and FS groups. (b) Total Cholesterol (TC) and Triglyceride (TG). (c) High-density lipoprotein cholesterol (HDL-C) and Low-Density Lipoprotein Cholesterol (LDL-C). (d) Alkaline phosphatase (ALP) and Creatine kinase (CK). (e) Total bilirubin (TBIL-V). (f) Phosphorus (P). (g) creatinine (CREA-S). * represents a significant difference between groups ($P < 0.05$), ** represents a significant difference between groups ($P < 0.01$), *** represents a significant difference between groups ($P < 0.001$).

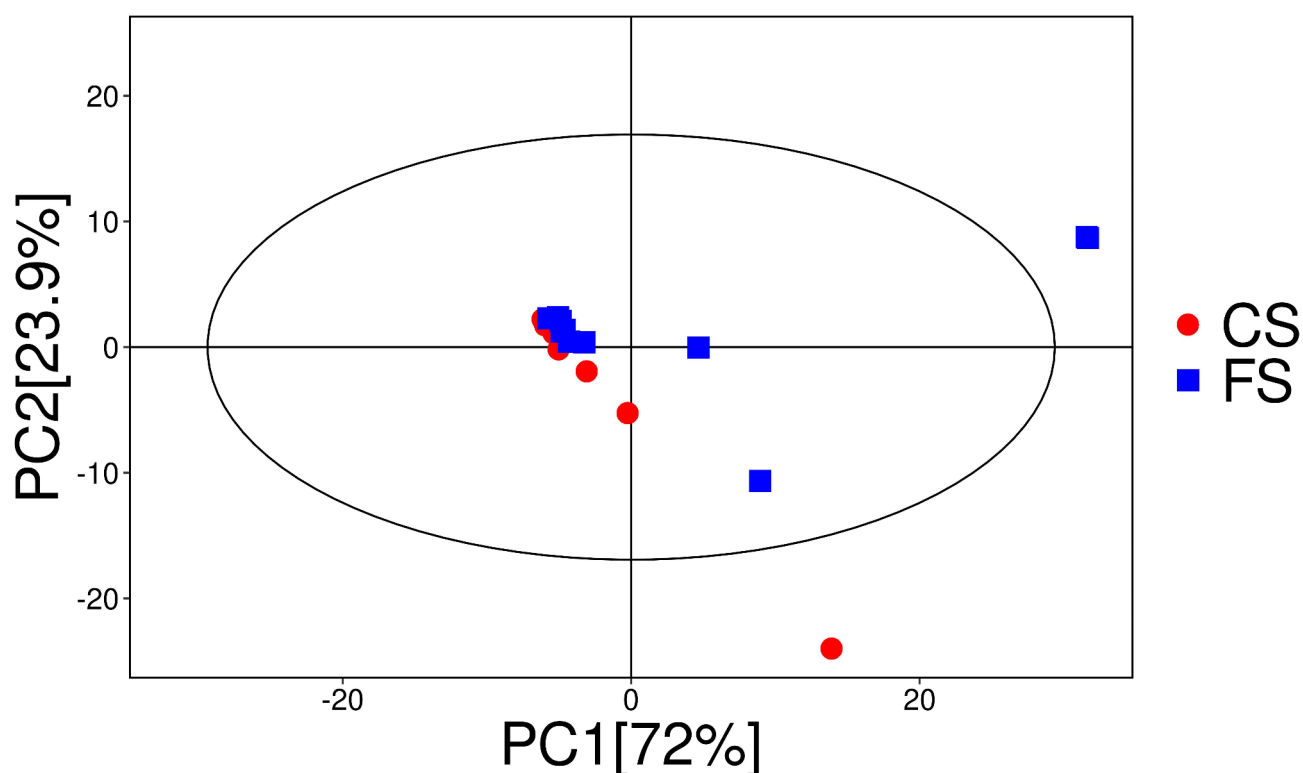


Fig. 2. Score scatter plot of PCA model for group CS versus FS.

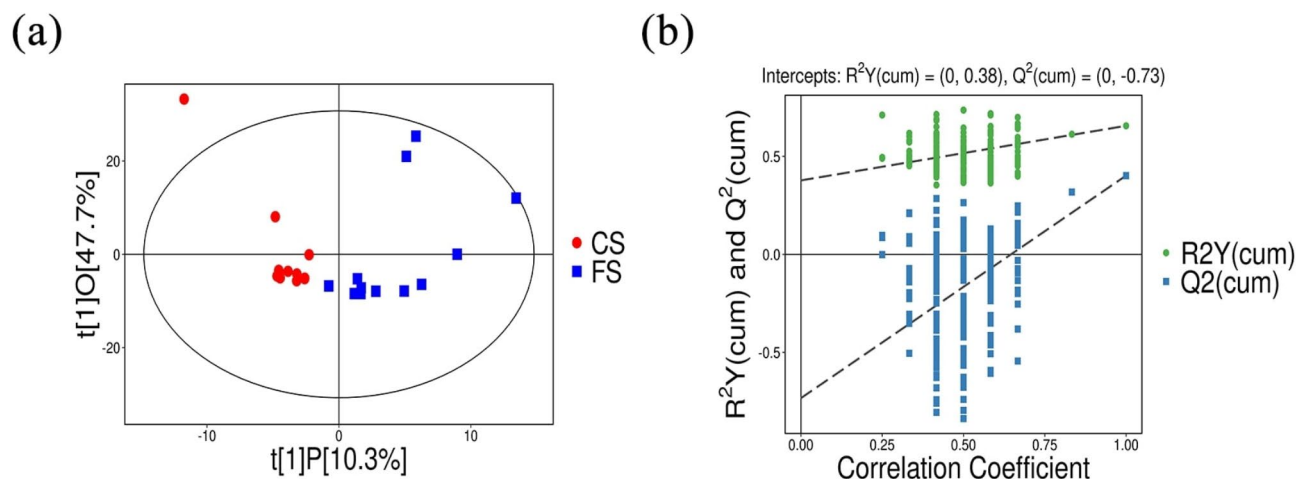


Fig. 3. Score scatter plot of OPLS-DA model for group CS versus FS. *Note:* (a) Score scatter plot of OPLS-DA model, the permutation retention of group CS (red) versus group FS (blue) permutation test is shown by abscission. (b) Permutation plot test of OPLS-DA model, the ordinate represents the value of R^2Y or Q^2 , and the two dashed lines represent the regression lines of R^2Y and Q^2 respectively.

decreased, both R^2Y and Q^2 of the random model decreased progressively. The permutation test revealed that the Q^2 value of the random model was smaller than that of the original model, and the intercept of the Q^2 regression line was negative, indicating absence of overfitting in the original model, allowing for subsequent experiments.

Screening of differential metabolites

We applied $VIP > 1$ and $P < 0.05$ as criteria to identify significantly different metabolites. Thirteen metabolites showed significant differences in serum between the CS and FS groups. The overall distribution was visualized using a Volcano Plot, presented in Fig. 4. Specifically, 2-HB, N-Methyl-DL-alanine, ornithine 1, Tagatose 1, Sedoheptulose and D-galacturonic acid 1 were upregulated, while Alpha-linolenic acid, D-(glycerol 1-phosphate), 4-aminophenol 2, Fluorene, 4-hydroxyphenylacetic acid, phthalic acid and alpha-D-glucosamine 1-phosphate were downregulated. These differential metabolites were classified and detailed in Table 1.

Enrichment analysis of differential metabolite metabolic pathways

We mapped the identified differential metabolites onto the KEGG database and conducted an enrichment analysis on the matched metabolic pathways. The results matched a total of 15 metabolic pathways, as shown in Fig. 5. Pathway enrichment analysis indicated that significant pathways involved in serum metabolism changes during the onset of FHL changes ABC transporters, choline metabolism in cancer, amino sugar and nucleotide sugar metabolism, among others. These findings are visually represented in a bubble chart (Fig. 6), highlighting enriched pathways such as glyceride metabolism, propionic acid metabolism, glutathione metabolism, glycerophospholipid metabolism, tyrosine metabolism, arginine and proline metabolism, the biosynthesis of unsaturated fatty acids, notably, alpha-linolenic acid metabolism was identified as a pivotal pathway strongly correlated with the observed metabolite differences.

ROC curve of differential metabolites

ROC analysis was performed on serum differential metabolites, as shown in Fig. 7. alpha linolenic acid, glycerophosphate, NG-methyl-L-arginine, L-ornithine, 4-aminophenol, fluorene, p-hydroxyphenylacetic acid, phthalic acid, D-tagatose, Sedum [ketohexose] sugar, and D-glucosamine 1-phosphate exhibited AUC values greater than 0.70, indicating diagnostic potential. Notably, galacturonic acid had an AUC value of 0.91, while 2-HB had an AUC value of 0.90, indicating high accuracy and strong diagnostic efficacy.

Changes in serum 2-HB levels in cats

As shown in Fig. 8a, the serum levels of 2-HB in the FS group were significantly higher than those in the CS group ($P < 0.001$, Fig. 8a). Furthermore, as illustrated in Fig. 8b, the ROC curve with an AUC of 0.90 (95% CI 0.767–1.000, $P < 0.001$). According to the Youden index calculation, the optimal cutoff value for diagnosing FHL is 564.8 ng/L, providing a sensitivity of 75% and specificity of 100%.

Validation of serum 2-HB as a biomarker for diagnosis of FHL

The results of the randomized sample test are summarized in Table 2. Using the optimal cutoff value of 564.8 ng/L for 2-HB, the diagnostic performance for FHL was evaluated, achieving a detection rate of 100% and a false positive rate of 0%.

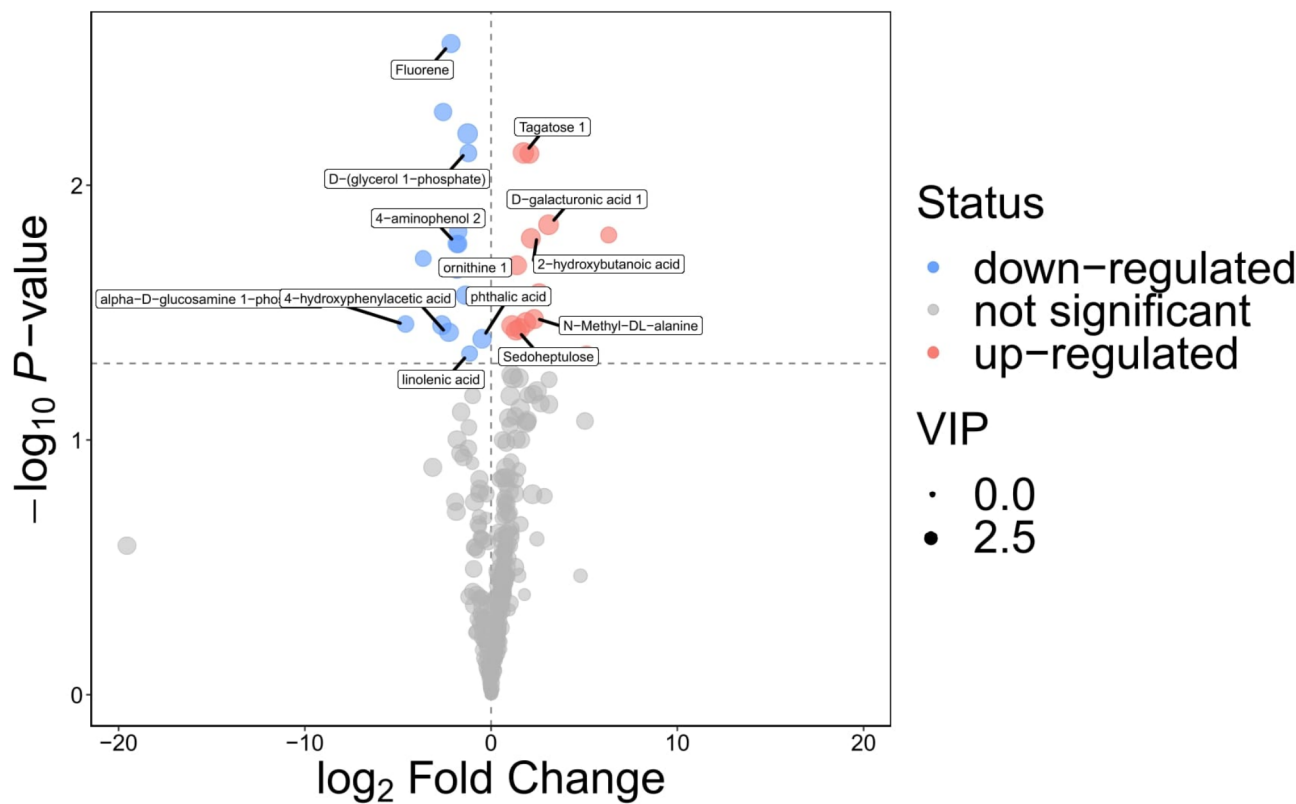


Fig. 4. Volcano plot for group CS versus FS. *Note:* The difference metabolites of up-regulation are shown in red, and the difference metabolites of downregulation are shown in blue.

NO.	Classify	Name of metabolite	VIP	P value	RT(s)	Change
1	Lipids and lipid-like molecules	2-hydroxybutyric acid	1.99	0.016	5.86	↑
2		Alpha-linolenic acid	1.03	0.046	12.31	↓
3		D-(glycerol 1-phosphate)	1.42	0.007	9.94	↓
4	Organic acids and derivatives	N-Methyl-DL-alanine	2.02	0.033	6.19	↑
5		Ornithine 1	1.93	0.021	10.27	↑
6	Benzenoids	4-aminophenol 2	1.49	0.017	9.10	↓
7		Fluorene	1.64	0.003	9.33	↓
8		4-hydroxyphenylacetic acid	1.79	0.038	9.34	↓
9		Phthalic acid	1.77	0.040	9.67	↓
10	Organic oxygen compounds	Tagatose 1	2.45	0.007	10.40	↑
11		Sedoheptulose	2.12	0.037	10.97	↑
12	Other class	D-galacturonic acid 1	2.21	0.014	10.86	↑
13		Alpha-D-glucosamine 1-phosphate	1.13	0.035	10.31	↓

Table 1. Gene-specific primers used in the present study. RT is the retention time of the metabolite on the chromatography; The content of “↑” group FS is higher than that of group CS, and “↓” group FS is lower than that of group CS.

Discussion

Serum biochemical indicators can reflect the lipid metabolism status in the liver, and FHL in cats can have an impact on it. This study observed significantly increased serum levels of TC and TG, extremely increased levels of LDL-C, and significantly reduced levels of HDL-C in the FS group. These findings are consistent with previous research on lipoproteins in cats with FHL, suggesting abnormal lipid metabolism and excessive hepatic accumulation in the liver⁸. Moreover, serum levels of ALT and AST were significantly elevated in the FS group, with slightly elevated gamma-glutamyl transferase (GGT), indicating liver cell damage and disrupted lipid metabolism. Further analysis underscores the intimate connection between lipid metabolism, liver pathology and changes in serum biochemical. Using GC-MS metabolomics, this study analyzed serum from cats in the

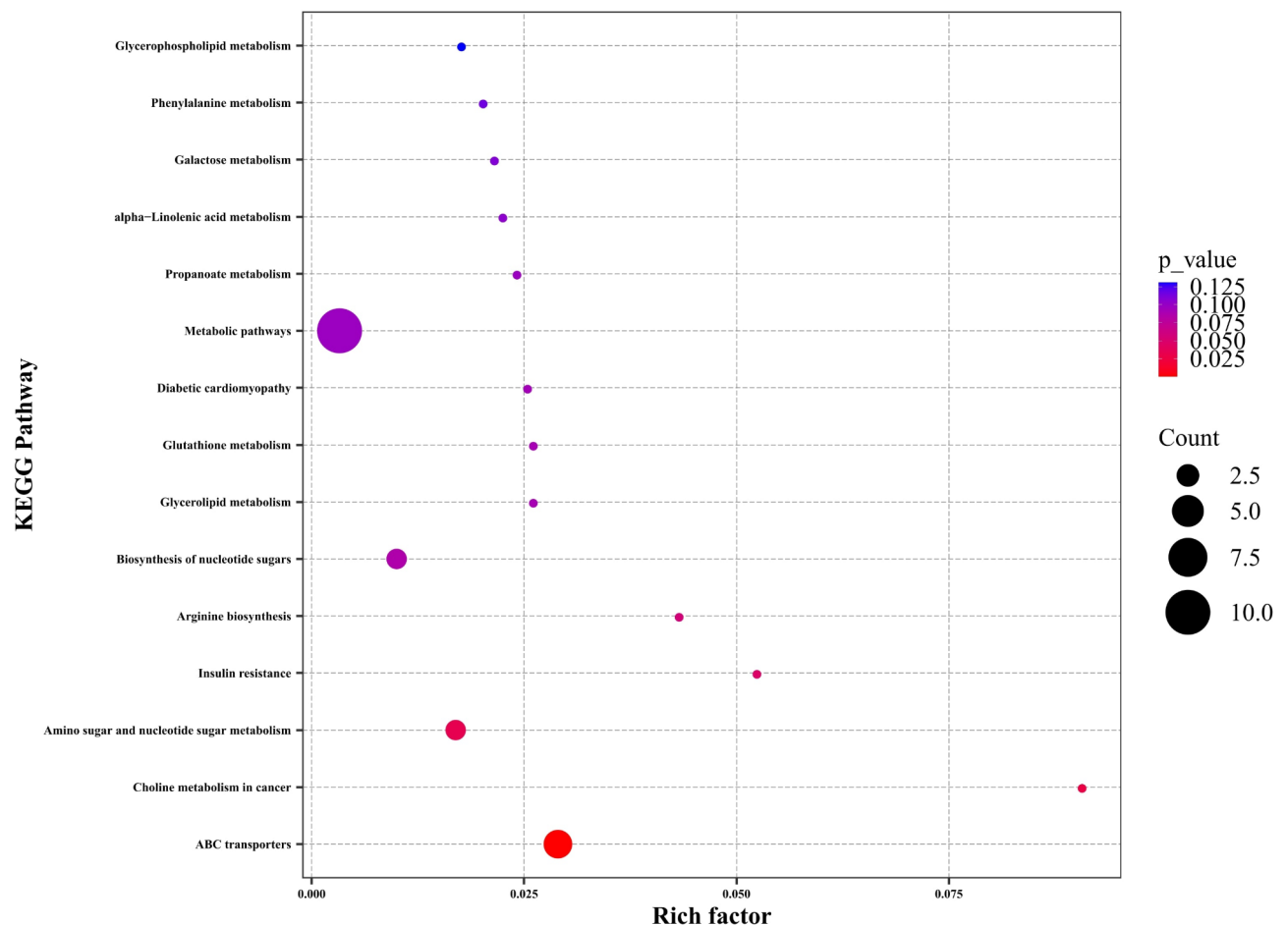


Fig. 5. KEGG enrichment map of differential metabolites between CS group and FS group. *Note:* The larger the value of the Rich Factor on the horizontal axis, the greater the degree of enrichment, and the size of the dots indicates the number of differential metabolites enriched in the pathway; The color represents the size of the P-value, and the smaller the P-value, the redder the color, indicating a more significant degree of enrichment.

control (CS) and FHL groups to explore metabolic alterations following FHL. Significant changes in certain serum metabolites in cats with FHL were identified, reflecting metabolic disorders closely associated with the onset and progression of FHL. These changes in lipids and lipid-like molecules may stem from disturbances in hepatic lipid synthesis and breakdown¹². Factors such as impaired liver function and reduced protein synthesis may lead to alterations in organic acids and derivatives¹³. An in-depth study found significant metabolite changes, especially in 2-HB, ALA, and D-glyceraldehyde-3-phosphate, crucial for FHL cat serum lipid metabolism.

Research indicates that human serum levels of 2-HB increase significantly with prolonged fasting; after 36 h of fasting, plasma 2-HB levels rise by 5.4 times¹⁴. During fasting, the beta-oxidation rate of free fatty acids (FFA) exceeds the capacity of acetyl CoA utilization in the tricarboxylic acid (TCA) cycle, leading to increased ketone production and subsequent changes in acid-base balance. α -Ketobutyric acid (α -KB) is converted to 2-HB catalyzed by lactate dehydrogenase (LDH)^{14–16}. Structurally similar to pyruvate, α -KB competes with it as a substrate for pyruvate dehydrogenase (PDH), potentially interfering with glucose metabolism^{13–15}. α -KB also inhibits pyruvate transport into mitochondria, reducing acetyl CoA synthesis and gluconeogenesis in rat liver cells^{16,17}. In patients with liver cirrhosis, saliva often shows elevated 2-HB levels, reflecting decreased mitochondrial metabolism¹⁷. Similarly, increased serum 2-HB during FHL may indicate reduced mitochondrial metabolic capacity in cats. 2-HB regulates body lipid metabolism by inhibiting de novo fatty acid synthesis, enhancing mitochondrial function, and promoting lipid hydrolysis¹⁸. According to this study, the optimal diagnostic cutoff for FHL using 2-HB is 564.8 ng/L. Levels exceeding this threshold may indicate enzyme activity damage or inhibition of mitochondrial enzyme expression, leading to reduced cell viability and proliferation¹⁹. Additionally, elevated 2-HB promotes mitochondrial division and cytochrome C release, triggering programmed cell death and exacerbating FHL progression. This correlates with increased serum TG levels and metabolic dysfunction in FHL cats^{19,20}. Low doses of 2-HB can enhance intracellular TG hydrolysis and reduce lipid accumulation by upregulating lipolytic protein expression in adipocytes^{18–20}. Higher serum 2-HB levels correlate with reduced cell viability, protein levels, and TNF- α , indicating liver cell damage and compromised cell membrane integrity, resulting in transaminase release into the bloodstream and elevated TG levels^{19–22}. Excessive lipid presence promotes inflammation, further exacerbating lipid accumulation; conversely, 2-HB

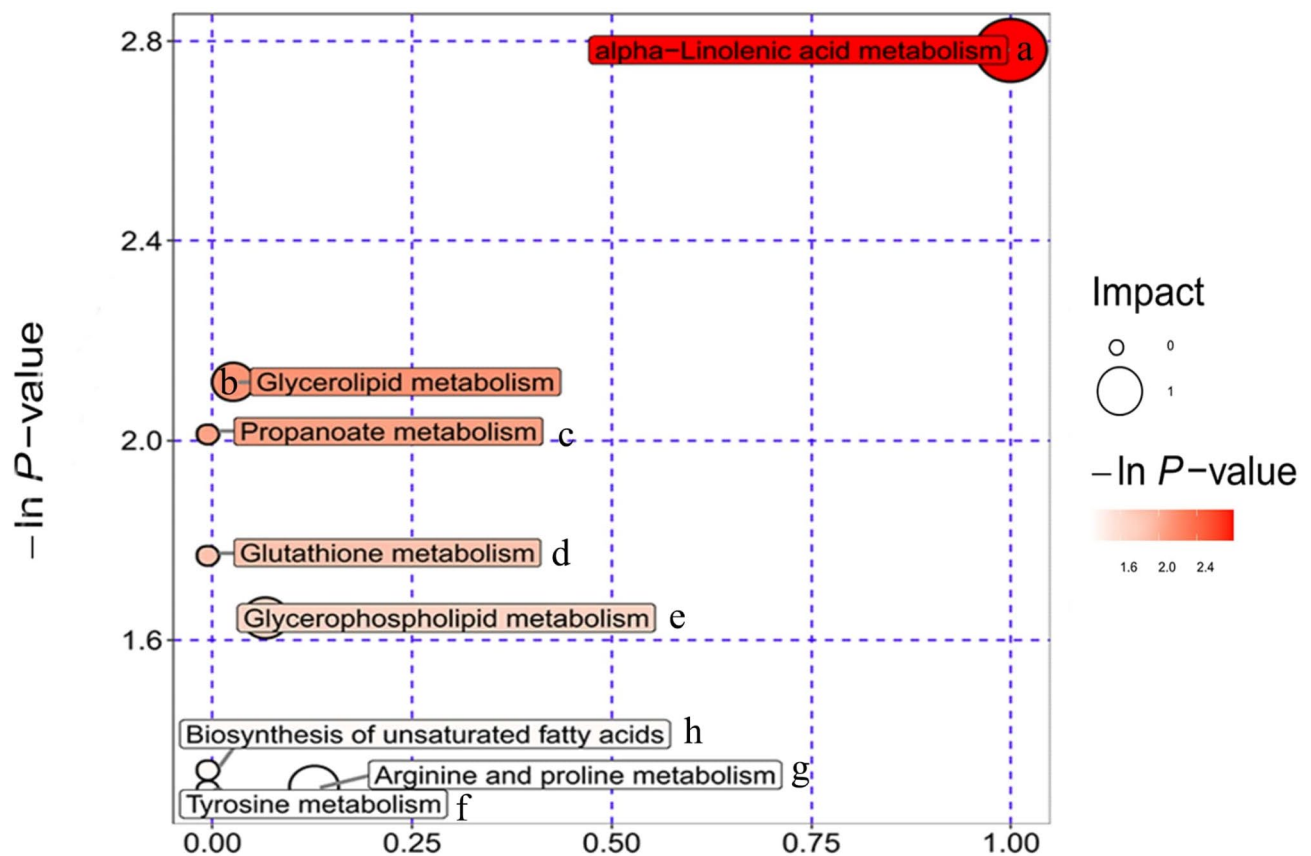


Fig. 6. Bubble map of metabolic pathway analysis results. *Note:* Each bubble in the figure represents a metabolic pathway, and the abscissa where the bubble is located and the size of the bubble indicate the size of the influencing factor of the pathway in topology analysis. The larger the size, the greater the influencing factor. (a) Alpha linolenic acid metabolism; (b) Glycerol ester metabolism; (c) Propionic acid metabolism; (d) Glutathione metabolism; (e) Glycerophospholipid metabolism; (f) Tyrosine metabolism; (g) Arginine and proline metabolism; (h) The biosynthesis of unsaturated fatty acids.

moderates inflammatory factors while reducing TG levels. In summary, decreased feline food intake accelerates β -oxidation rates beyond acetyl CoA utilization, increasing protein hydrolysis and prolonging fasting-induced serum 2-HB elevation^{2,23,24}.

Our study conducted KEGG analysis on differential metabolites, identifying 15 matched metabolic pathways. Pathway enrichment analysis highlighted key pathways affected during FHL, including ABC transporters, choline metabolism in cancer, and amino sugar and nucleotide sugar metabolism. Among these, ALA metabolism emerged as the pathway most significantly correlated with metabolite variations. Notably, ALA levels were significantly reduced in the serum of cats with FHL²⁵. ALA, an essential free fatty acid in mammals, cannot be synthesized endogenously and must be obtained through dietary sources^{20,26,27}. ALA is pivotal in inhibiting adipocyte differentiation and proliferation, reducing fat synthesis, and alleviating the impact of chronic inflammation on metabolic disorders related to lipid accumulation through its anti-inflammatory effects²⁸. Furthermore, it may aid in weight management by enhancing satiety, decreasing high-calorie food intake, and optimizing energy balance. Research also suggests that ALA boosts carnitine palmitoyltransferase activity, thereby facilitating fatty acid oxidation²⁹. Supplementation with fish oil, rich in ALA, has been shown to inhibit fatty acid synthase and acetyl CoA carboxylase activity, lowering serum TG, TC, and LDL-C levels, while elevating HDL-C levels in animals^{30–32}. In FHL, low dietary intake causes ALA deficiency, which affects β -oxidation and fat metabolism, and reduces cholesterol and bile acid excretion. This leads to increased hepatic fatty acid synthesis and lower decreased lipoprotein lipase (LPL) expression and activity, resulting in higher plasma TG and low-density lipoprotein: VLDL levels, and impacting liver cholesterol metabolism^{31–33}. This study underscores that during FHL, decreased dietary ALA intake exacerbates increases in serum TG, TC, and LDL-C levels, alongside decreased HDL-C levels. Introducing appropriate ALA supplementation in the diet may potentially aid in FHL recovery, though further clinical trials are necessary to validate this hypothesis.

Conclusion

Thirteen significantly differentially expressed metabolites in cat serum are implicated in the onset of FHL. Pathway enrichment analysis revealed their involvement in key metabolic pathways such as ABC transporters, choline

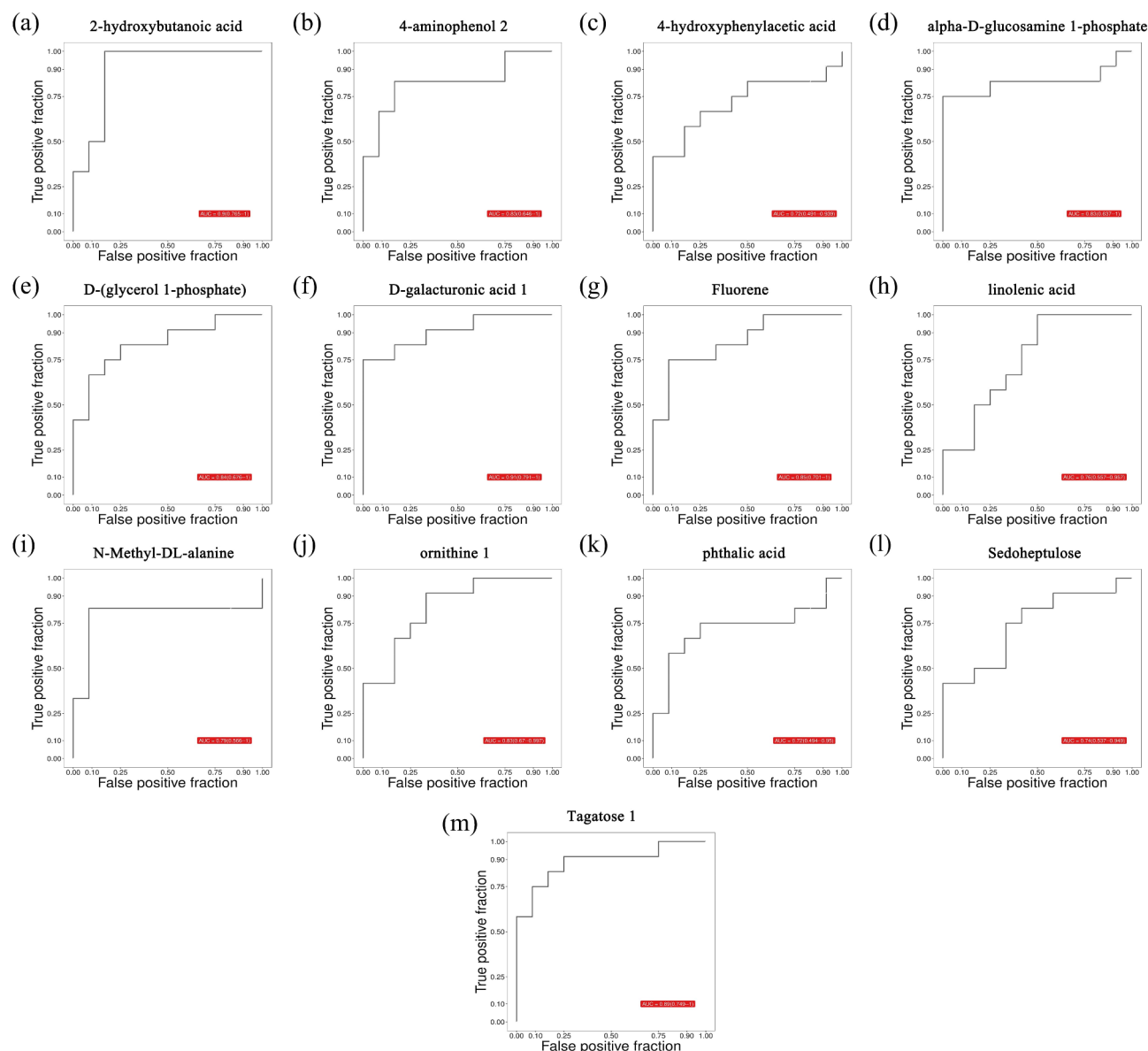


Fig. 7. ROC curve of differentially expressed metabolites. *Note:* (a) is the ROC curve of 2-hydroxybutyric acid. (b) 4-aminophenol 2. (c) 4-hydroxyphenylacetic acid. (d) alpha-D-glucosamine 1-phosphate. (e) D-(glycerol 1-phosphate). (f) D-galacturonic acid 1. (g) Fluorene. (h) linolenic acid. (i) N-Methyl-DL-alanine. (j) ornithine 1. (k) phthalic acid. (l) Sedoheptulose. (m) Tagatose 1. Area Under the Curve (AUC) is the area under the ROC curve.

metabolism in cancer, amino acid and nucleotide sugar metabolism. Additionally, enriched metabolic pathways include glyceride metabolism, propionic acid metabolism, glutathione metabolism, glycerophospholipid metabolism, tyrosine metabolism, arginine and proline metabolism. Among these metabolites, serum 2-HB levels serve as a risk indicator for FHL, exhibiting an area under the curve (AUC) of 0.90. The identified warning threshold for 2-HB is 564.8 ng/L, demonstrating a sensitivity of 75%, and specificity of 100%.

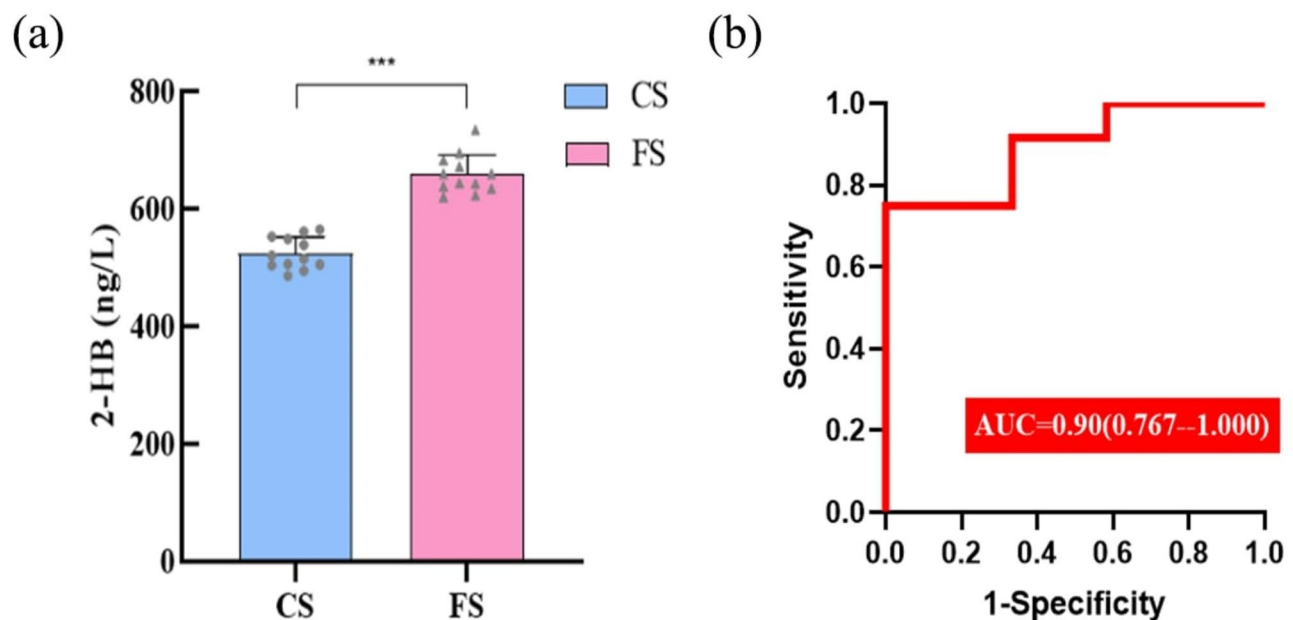


Fig. 8. 2-HB as a diagnostic biomarker for FHL. *Note:* (a) Levels of 2-HB in serum in Group CS and Group FS, *** represents a significant difference between groups ($P < 0.001$). (b) The ROC analysis results of serum 2-HB on FHL.

	FHL(+)	FHL(-)	Total
Diagnosis results of liver biopsy	10	50	60
Diagnosis of serum 2-HB cutoff value (> 564.8 ng/L)	10	50	60
Detection rate	100%		
False positive rate		0%	

Table 2. The diagnostic accuracy of optimal thresholds of 2-HB for FHL after ROC curve evaluation. FHL is Feline Hepatic Lipidosis, FHL (+) indicates the number of cats with feline hepatic steatosis, whereas FHL (-) indicates the number of cats without feline hepatic steatosis.

Data availability

All data generated or analyzed during this study are included in the published article.

Received: 20 November 2024; Accepted: 24 February 2025

Published online: 06 March 2025

References

- Rochus, K., Janssens, G. P. & Hesta, M. Dietary fibre and the importance of the gut microbiota in feline nutrition: A review. *Nutr. Res. Rev.* **27**(2), 295–307. <https://doi.org/10.1017/s0954422414000213> (2014).
- Webb, C. B. Hepatic lipidosis: Clinical review drawn from collective effort. *J. Feline Med. Surg.* **20**(3), 217–227. <https://doi.org/10.1177/1098612x18758591> (2018).
- Valtolina, C. & Favier, R. P. Feline hepatic lipidosis. *Vet. Clin. North. Am. Small Anim. Pract.* **47**(3), 683–702. <https://doi.org/10.1016/j.cvsm.2016.11.014> (2017).
- Jin, Q. & Ma, R. C. W. Metabolomics in diabetes and diabetic complications: Insights from epidemiological studies. *Cells* **10**(11), 2832. <https://doi.org/10.3390/cells10112832> (2021).
- Colyer, A. et al. Identification of intra- and inter-individual metabolite variation in plasma metabolite profiles of cats and dogs. *Br. J. Nutr.* **106**(Suppl 1), S146–S149. <https://doi.org/10.1017/s000711451100081x> (2011).
- Krasztel, M. M. et al. Correlation between metabolomic profile constituents and feline pancreatic lipase immunoreactivity. *J. Vet. Intern. Med.* **36**(2), 473–481. <https://doi.org/10.1111/jvim.16349> (2022).
- Deng, P., Jones, J. C. & Swanson, K. S. Effects of dietary macronutrient composition on the fasted plasma metabolome of healthy adult cats. *Metabolomics* **10**, 638–650. <https://doi.org/10.1007/s11306-013-0617-7> (2014).
- Pallotto, M. R. et al. Effects of weight loss and moderate-protein, high-fiber diet consumption on the fasted serum metabolome of cats. *Metabolites* **11**(5), 324. <https://doi.org/10.3390/metabo11050324> (2021).
- Zhao, C. et al. Metabolic alterations in dairy cows with subclinical ketosis after treatment with carboxymethyl chitosan-loaded, reduced glutathione nanoparticles. *J. Vet. Intern. Med.* **34**(6), 2787–2799. <https://doi.org/10.1111/jvim.15894> (2020).
- Dunn, W. B. et al. Procedures for large-scale metabolic profiling of serum and plasma using gas chromatography and liquid chromatography coupled to mass spectrometry. *J. Nat. Protocols.* **6**(7), 1060–1083. <https://doi.org/10.1038/nprot.2011.335> (2011).
- Jolliffe, I. *Principal Component Analysis*. (Wiley Online Library, 2002). <https://doi.org/10.1002/0470013192.bsa501>

12. Ter Horst, K. W. & Serlie, M. J. Fructose consumption, lipogenesis, and non-alcoholic fatty liver disease. *Nutrients* **9**(9), 981. <https://doi.org/10.3390/nu9090981> (2017).
13. Hodson, L., Rosqvist, F. & Parry, S. A. The influence of dietary fatty acids on liver fat content and metabolism. *Proc. Nutr. Soc.* **78**(3), 473. <https://doi.org/10.1017/s0029665119000697> (2019).
14. Raclot, T. & Oudart, H. Selectivity of fatty acids on lipid metabolism and gene expression. *Proc. Nutr. Soc.* **58**(3), 633–646. <https://doi.org/10.1017/s002966519900083x> (1999).
15. Rubio-Aliaga, I. et al. Metabolomics of prolonged fasting in humans reveals new catabolic markers. *Metabolomics* **7**, 375–387. <https://doi.org/10.1007/s11306-010-0255-2> (2011).
16. Miyazaki, T. et al. Simultaneous quantification of salivary 3-hydroxybutyrate, 3-hydroxyisobutyrate, 3-hydroxy-3-methylbutyrate, and 2-hydroxybutyrate as possible markers of amino acid and fatty acid catabolic pathways by LC-ESI-MS/MS. *Springerplus* **4**, 494. <https://doi.org/10.1186/s40064-015-1304-0> (2015).
17. Paradies, G. & Papa, S. The transport of monocarboxylic oxoacids in rat liver mitochondria. *FEBS Lett.* **52**(1), 149–152. [https://doi.org/10.1016/0014-5793\(75\)80659-4](https://doi.org/10.1016/0014-5793(75)80659-4) (1975).
18. Tricò, D. et al. Elevated α -hydroxybutyrate and branched-chain amino acid levels predict deterioration of glycemic control in adolescents. *J. Clin. Endocrinol. Metab.* **102**(7), 2473–2481. <https://doi.org/10.1210/je.2017-00475> (2017).
19. Stryeck, S. et al. Serum concentrations of citrate, tyrosine, 2- and 3-Hydroxybutyrate are associated with increased 3-Month mortality in acute heart failure patients. *Sci. Rep.* **9**(1), 6743. <https://doi.org/10.1038/s41598-019-42937-w> (2019).
20. Miotto, P. M. et al. α -Linolenic acid supplementation and exercise training reveal independent and additive responses on hepatic lipid accumulation in obese rats. *Am. J. Physiol. Endocrinol. Metab.* **312**(6), E461–E470. <https://doi.org/10.1152/ajpendo.00438.2016> (2017).
21. Verbrugghe, A. & Bakovic, M. Peculiarities of one-carbon metabolism in the strict carnivorous cat and the role in feline hepatic lipidosis. *Nutrients* **5**(7), 2811–2835. <https://doi.org/10.3390/nu5072811> (2013).
22. Sousa, A. P. et al. Which role plays 2-hydroxybutyric acid on insulin resistance? *Metabolites* **11**(12), 835 (2021). <https://doi.org/10.3390/metabo11120835>
23. Adams, L. G. et al. Hypophosphatemia and hemolytic anemia associated with diabetes mellitus and hepatic lipidosis in cats. *J. Vet. Intern. Med.* **7**(5), 266–271. <https://doi.org/10.1111/j.1939-1676.1993.tb01018.x> (1993).
24. Mazaki-Tovi, M., Abood, S. K., Segev, G. & Schenck, P. A. Alterations in adipokines in feline hepatic lipidosis. *J. Vet. Intern. Med.* **27**(2), 242–249. <https://doi.org/10.1111/jvim.12055> (2013).
25. Goyens, P. L. L. et al. Conversion of alpha-linolenic acid in humans is influenced by the absolute amounts of alpha-linolenic acid and Linoleic acid in the diet and not by their ratio. *Am. J. Clin. Nutr.* **84**(1), 44–53. <https://doi.org/10.1093/ajcn/84.1.44> (2006).
26. Anderson, B. M. & Ma, D. W. Are all n-3 polyunsaturated fatty acids created equal? *Lipids Health Dis.* **8**, 33. <https://doi.org/10.1186/1476-511x-8-33> (2009).
27. Dominguez, T. E., Kaur, K., Burri, L. & Enhanced omega-3 index after long-versus short-chain omega-3 fatty acid supplementation in dogs. *Vet. Med. Sci.* **7**(2), 370–377. <https://doi.org/10.1002/vms3.369> (2021).
28. Wang, M. et al. Dietary α -linolenic acid-rich flaxseed oil prevents against alcoholic hepatic steatosis via ameliorating lipid homeostasis at adipose tissue-liver axis in mice. *Sci. Rep.* **6**, 26826. <https://doi.org/10.1038/srep26826> (2016).
29. Nieves, D. J. et al. The atherogenic lipoprotein profile associated with obesity and insulin resistance is largely attributable to intra-abdominal fat. *Diabetes* **52**(1), 172–179. <https://doi.org/10.2337/diabetes.52.1.172> (2003).
30. Greco, D. S. Nutritional supplements for pregnant and lactating bitches. *Theriogenology* **70**(3), 393–396. <https://doi.org/10.1016/j.theriogenology.2008.04.013> (2008).
31. Hall, J. A. et al. Influence of dietary long-chain n-3 fatty acids from menhaden fish oil on plasma concentrations of alpha-tocopherol in geriatric Beagles. *Am. J. Vet. Res.* **63**(1), 104–110. <https://doi.org/10.2460/ajvr.2002.63.104> (2002).
32. Hall, J. A. et al. Increased dietary long-chain polyunsaturated fatty acids alter serum fatty acid concentrations and lower risk of urine stone formation in cats. *PLoS One* **12**(10), e0187133. <https://doi.org/10.1371/journal.pone.0187133> (2017).
33. Wang, Q. & Wang, X. The effects of a low Linoleic acid/ α -Linolenic acid ratio on lipid metabolism and endogenous fatty acid distribution in obese mice. *Int. J. Mol. Sci.* **24**(15), 12117. <https://doi.org/10.3390/ijms241512117> (2023).

Author contributions

C. Z. completed the experimental design, and manuscript writing. X.W. and We. Y. completed the sample collection work and animal sample detection. K.W. and R. X. completed the animal feeding. S.F., X. W., and H. D. provided good design ideal for the experiment and made language modifications to the manuscript.

Funding

This study was supported by the National Science Foundation of China (Grant No: 3220190315). We would like to express our gratitude to Anhui Agricultural University Teaching Animal Hospital, Daqing Renxin Pet Hospital, and Daqing Kang'an Pet Hospital for their kind provision of FHL serum samples.

Declarations

Competing interests

The authors declare no competing interests.

Ethics approval

This study was conducted in accordance with the ARRIVE guidelines (<https://arriveguidelines.org>) to ensure rigorous standards in animal research reporting. All procedures were performed following relevant ethical guidelines and regulations. The study was approved by the Animal Welfare and Research Ethics Committee of Anhui Agricultural University, China (Approval Number: 2021012-1).

Experiments and analysis compliance with ethical standards

This study is reported in accordance with ARRIVE guidelines. Ethical standards were respected. The management of all animals adhered to the standards approved by the Ethics Committee for Animal Welfare and Research of Anhui Agricultural University, China (Approval Number: 2021012-1).

Additional information

Supplementary Information The online version contains supplementary material available at <https://doi.org/10.1038/s41598-025-91770-x>

[0.1038/s41598-025-91770-x](https://doi.org/10.1038/s41598-025-91770-x).

Correspondence and requests for materials should be addressed to C.Z.

Reprints and permissions information is available at www.nature.com/reprints.

Publisher's note Springer Nature remains neutral with regard to jurisdictional claims in published maps and institutional affiliations.

Open Access This article is licensed under a Creative Commons Attribution-NonCommercial-NoDerivatives 4.0 International License, which permits any non-commercial use, sharing, distribution and reproduction in any medium or format, as long as you give appropriate credit to the original author(s) and the source, provide a link to the Creative Commons licence, and indicate if you modified the licensed material. You do not have permission under this licence to share adapted material derived from this article or parts of it. The images or other third party material in this article are included in the article's Creative Commons licence, unless indicated otherwise in a credit line to the material. If material is not included in the article's Creative Commons licence and your intended use is not permitted by statutory regulation or exceeds the permitted use, you will need to obtain permission directly from the copyright holder. To view a copy of this licence, visit <http://creativecommons.org/licenses/by-nc-nd/4.0/>.

© The Author(s) 2025